

10. DIAGENETIC DOLOMITE FORMATION IN QUATERNARY ANOXIC DIATOMACEOUS MUDS OF DEEP SEA DRILLING PROJECT LEG 64, GULF OF CALIFORNIA¹

Kerry Kelts and Judith A. McKenzie, Eidgenössische Technische Hochschule, Geologisches Institut, Zürich, Switzerland

ABSTRACT

During drilling in the Gulf of California, diagenetic carbonate rocks were recovered at 7 out of 8 sites. These are primarily dolomites which record ¹³C isotopic evidence of the incorporation of carbon derived from the decomposition of organic matter. In Hole 479, drilled to a sub-bottom depth of 440 meters on the Guaymas Slope, under a fertile upwelling belt, we recognized an excellent example of deep sea dolomitization in progress. This Quaternary section of organic-carbon-rich, low-carbonate, hemipelagic diatomaceous oozes contains numerous fine-grained, decimeter-thin, episodic beds of dolomite, which show sedimentologic, geochemical, and isotopic evidence of accretion by precipitation below 40 meters sub-bottom in zones of high alkalinity and low sulfate. The beds preserve original sedimentary structures. Carbon-13 varies from +3 to +14‰, indicating biogenic CO₂ reservoirs related to active methanogenesis. In single beds, ¹⁸O values range outwardly from +5 to -7‰, reflecting increasing temperature with progressive accretion of dolomite with depth; the values parallel progressive trends in lithification, texture, mineralogy, and fossil preservation. We estimate slow accretion rates on the order of 0.1-0.7 mm/10³ yr. with burial. Dolomitization does not proceed merely at the expense of nearby nanofossils. Ca and Mg ions must be derived from interstitial waters. The episodic appearance of beds in the sequence seems partly a reflection of latent climate signals. This process of deep sea dolomitization carries implications for hydrocarbon migration, as well as an interpretation of the presence of dolomite in other modern and ancient pelagic to hemipelagic sediment sequences.

INTRODUCTION

Land (1980), in a review of dolomite formation, concluded that there is no unique environment for this process. Thus, in our quest for a unifying principle, unusual rather than common occurrences may provide the best clues. An association of dolomite with sediments rich in organic matter has long been known from the geologic record (e.g., Bramlette, 1946). Numerous stable-isotope investigations of diagenetic dolomite concretions and beds associated with deep sea sediments indicate that biogenic CO₂ related to bacterial sulfate reduction and methanogenesis participates in the reaction (Spotts and Silverman, 1966; Russell et al., 1967; Hathaway and Degen, 1969; Murata et al., 1969; Deuser, 1970; Irwin et al., 1977; Hein et al., 1979; Friedman and Murata, 1979; McKenzie et al., 1980; Kelts and McKenzie, 1980; Pisciotto and Mahoney, 1981; Pisciotto, 1981; and Irwin, 1981). Claypool and Kaplan (1974) derived a predictive model for the isotopic signature of carbonates precipitated in conjunction with methane generation in sediments. Our survey of 19 occurrences of dolomite reported in DSDP *Initial Reports* showed that 16 occurred in association with sediments rich in organic matter, although most were interpreted as products of hypersaline brines or redeposition (e.g., Supko et al., 1974; Berger and von Rad, 1972).

The impetus for a reconsideration of the role of reducing environments in dolomite formation (e.g., Baker and Kastner, 1981) derives partly from the discovery, during DSDP Legs 63 and 64, of extensive diagenetic

dolomites in anoxic hemipelagic, diatomaceous muds along the continental margin of California, Baja California, and the Gulf of California (Pisciotto and Mahoney, 1981; Kelts and McKenzie, 1980). These areas are paleoenvironmental equivalents to the Monterey Formation of California and other Neogene circum-Pacific deposits where biogenic silica and intercalated dolomite layers are also associated. Such deposits are currently being reexamined for their hydrocarbon potential (Friedman and Murata, 1979; Garrison, 1981).

This paper reports the sedimentological, petrological, and isotopic data from a survey of diverse diagenetic carbonate samples recovered at 7 out of 8 sites drilled during DSDP Leg 64 in the Gulf of California (Fig. 1). The analysis focuses in particular on progressive trends of dolomitization in Hole 479, which provides an excellent case study for Quaternary dolomitization in progress in the deep sea environment.

The Quaternary setting and paleoenvironment at Site 479 are well defined, and *in situ* conditions are controlled by interstitial water geochemistry (Gieskes et al., this volume, Pt. 2), organic geochemistry (Simoneit et al., summary, this volume, Pt. 2), and isotopic composition of gases and water (Schoell, this volume, Pt. 2, and Galimov and Simoneit, this volume, Pt. 2). We attempt to approach questions of where, when, and how dolomite forms in the Gulf of California sediments, although the question of why remains open.

METHODS

An interpretation of isotopic signatures in dolomitic rocks requires a knowledge of the detailed sedimentology and sediment petrology of the analyzed samples. We noted macroscopic features and primary sedimentary structures from core surfaces and slabs. Microtextures were studied with thin sections and by scanning electron microscopy (SEM) on clean, broken surfaces. We examined bulk and carbonate

¹ Curray, J. R., Moore, D. G., et al., *Init. Repts. DSDP, 64*; Washington (U.S. Govt. Printing Office).

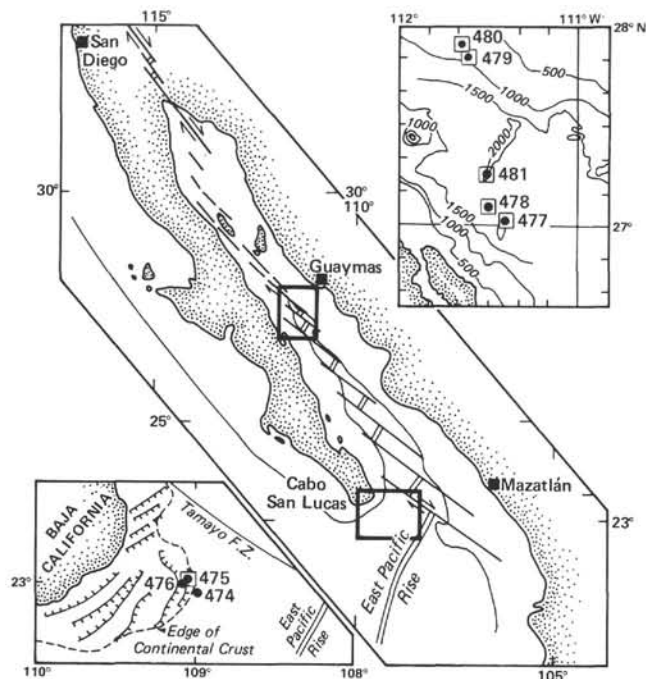


Figure 1. Location map for Sites 474-481, Gulf of California. Squares indicate sites with diagenetic dolomite.

mineralogy using smear slides, SEM with energy dispersion analysis, and a calibrated Phillips X-ray diffraction unit (XRD) using $\text{CuK}\alpha$, Ni-filtered radiation (Table 1). Selected samples were subjected to various dissolution, sieving, and settling experiments and clay mineral analysis. Carbonate percentages are derived from shipboard Carbonate Bomb results and shore-based LECO carbon analysis (Simoneit and Bode, this volume, Pt. 2). Additional determinations of total carbon for our samples were made with a Coulomat carbon analyzer which automatically titrates CO_2 in a solution produced by heating 100 mg of powdered sample to 1300°C in a stream of pure oxygen. Analyses are reproducible to 0.1% C_{org} (Table 2).

Spot analysis on 10 thin sections from well-lithified samples were performed with an ARL-SEQM microprobe at 15 kV for the elements Ca, Mg, Fe, Si, Al, Na, K, and Mn. Corrections were made for ZAF and frequent standardization indicated a very stable beam. The quantitative evaluation of these measurements is, however, hampered by the small crystal sizes, inclusions, and lack of precise CO_2 compositions (Table 3).

Carbon-13 and oxygen-18 isotopic ratios were measured simultaneously on a Micromass 903 triple collector mass spectrometer on CO_2 gas samples prepared from the carbonate using the traditional phosphoric acid method (McCrea, 1950) after the removal of any organic matter by oxidation with a 6% sodium hypochlorite solution. Appropriate correction factors were applied (Craig, 1957) on results expressed as per mil deviations from the PDB isotopic standard:

$$\delta = [(R_{\text{sample}}/R_{\text{standard}}) - 1] \times 10^3$$

where $R = {}^{13}\text{C}/{}^{12}\text{C}$ or ${}^{18}\text{O}/{}^{16}\text{O}$. The measurements are very precise: a standard deviation of the mean calculated for replicate analysis is $\pm 0.08\%$ for $\delta^{13}\text{C}$ and $\pm 0.10\%$ for $\delta^{18}\text{O}$. A value of 0.8‰ is subtracted from dolomite ${}^{18}\text{O}$ values to account for the acid-fractionation difference relative to that for calcite (Sharma and Clayton, 1965). Most samples contained nonstoichiometric dolomite, but no corrections were applied for anomalous magnesian contents. Results of stable isotope analyses are listed in Table 1.

SITE 479

Site 479 was drilled to 440 meters sub-bottom in 766 meters of water on the outer marginal slopes of the

Guaymas Basin (Fig. 1). This site was initially selected for its present-day location beneath an upwelling zone of fertile waters with prolific seasonal blooms of diatoms and dinoflagellates and a corresponding underlying layer of low-oxygen water, which intersects the slope between about 500 and 1300 meters (Calvert, 1966). It is not surprising that the sediment column (Fig. 2) consists mostly of olive-drab, rapidly deposited, anoxic, hemipelagic, muddy diatomaceous oozes, rich in organic carbon. Most of the section suffered badly from drill disturbance and gas exsolution features. Few of the carbonate samples were recovered intact with their contact zones preserved. Traces of original bedding and a comparison with the nearby HPC-cored Site 480 lead us to surmise that the oozes are generally organized into alternating meter-thick zones with rhythmic, varvelike laminations and zones which are homogeneous to faintly banded (see site chapter, Sites 479-480, this volume, Pt. 1). Accumulation rates are extremely high, estimated to be from about 220 to 600 m/m.y., or about 0.5 mm/yr.

The section (Fig. 2) reflects generally uniform conditions throughout the cored intervals but is divided into 3 sedimentary units on the basis of two breaks in sedimentation that might mark hiatuses: (1) a coarse sand layer in Core 479-26 (240 m), and (2) a change in sediment induration which accompanies increased compaction and the disappearance of biogenic silica in laminated mudstones below Core 479-40 (364 m; see Fig. 3). Ultra-fine laminations characterize this lower olive gray claystone. Partings contain kerogen and sparkling fish scales, and a few lamellae constitute a monospecific coccolith ooze (see site chapter, this volume, Pt. 1). These features suggest that this lower unit was similar to the diatomaceous oozes above, but that biogenic opal has been removed diagenetically. The hiatus may cover several hundred thousand years, judging by a late Pliocene foraminiferal fauna that occurs below (Matoba and Oda, this volume, Pt. 2).

Sporadic, hard dolomitic fragments and decimeter-thin beds occur within softer oozes to mudstones in all three units. The first bed was encountered at 88 meters below the sediment/water interface in Core 479-10, and others follow episodically at spaced intervals. Using logging results (Fig. 2) we could clearly identify the presence of at least 19 lithified horizons which are initially spaced at about 20 meters apart, and then at about 5-10 meters apart below 350 meters, partly as a result of increasing compaction. Individual beds do not appear to be larger than about 30-40 cm; hard dolomitic layers therefore account for a maximum of only 2-3% of the sedimentary section. At present, we do not know the lateral extent of these horizons, or if some are concretionary. However, no concentric structures were observed, and we assume, by analogy with Neogene outcrops of the Monterey Formation, that beds pinch and swell but have kilometer-range continuity (Bramlette, 1946; Pisciotto, 1981). Larger samples are fine-grained micritic rocks with color hues from yellowish to olive gray. The color mottles outline preserved primary sediment structures which indicate that the dolomite formed

Table 1. Results of carbon and oxygen isotope analyses correlated with lithology and bulk carbonate mineralogy.

Sample (interval in cm)	Lithology/ Induration	$\delta^{18}\text{O}$	$\delta^{13}\text{C}$	Bulk X-ray Mineralogy (relative major peaks in mm height)				Observations
				Dolomite	Calcite	Quartz	% Mg in Dolomite	
Hole 479								
10-6, 130*	Firm to hard lumps	+3.02	+7.50	111	18	7	48	Broad mixed-layer clay peaks
16-2, 38	Hard fragments	+5.08	+11.26	98	—	25		
20-1, 100*	Light-colored piece	+4.20	+12.86	192	—	4	48	
20-3, 65*	Light-colored piece	+3.66	+13.78	202	—	5	48	
23-1, 73*	Yellow flakes in ooze	+0.79	+12.94	89	6	11	47	
29-1, 1.5	Soft	-2.15	+11.54	214	—	31	46	
29-1, 4.5	Friable	-0.41	+12.47	260	—	22	48	
29-1, 11	Hard, brittle, massive	+2.66	+11.96	280	—	14	46	
29-1, 15*	Laminated, hard	+2.78	+11.64	280	—	15	48	
29-1, 15b	Laminated, hard	+3.51	+11.35					
29-1, 24.5	Soft chips	-0.39	+11.56	250	—	31	48	
29-1, 26.5	Soft ooze	-1.04	+11.01	168	—	53	47	
29,CC*	Laminated, hard	+4.25	+7.26	139	trace	7	45	
32,CC*		+3.74	+13.13	170	—	4	49	
34-5, 148	Friable, massive	+0.33	+11.68	238	—	22	48	
39-1, 37*	Laminated, soft	-0.99	+11.13	119	—	7	50	Broad, low I_{dolomite}
41-1, 134	Massive, light	+4.00	+6.25	174	—	3		
44-3, 142*	Crumbly, light	-2.67	+0.14	3	13	25	48	Contains foraminifers
45,CC*	Laminated, soft	-5.76	+5.20	66	—	35	44	Low I_{dolomite} 211
47-1, 35*		+2.65	+11.40	75	—			
47-2, 126*	Laminated, soft	-7.64	+3.52	75	—		42	
47-2, 129.5		-4.75	+5.46					
47-2, 132*		-0.46	+8.68					
47-2, 135*	Laminated, hard	+2.90	+10.44	167	—	13	51	
47-2, 139*	Massive, hard	+2.32	+11.07	179	2	8	51	Contains Mg-calcite
47-2, 148*	Massive, hard	+3.08	+11.50	189	—	13		
Hole 480								
21-1, 32*	Massive, friable	+3.99	+1.53	90	10			
Hole 478								
1-1, 50	Mollusk shells	+3.27	-1.27	Pure aragonite				
5-1, 130	Firm yellow lumps	+6.60	+4.70	Magnesium calcite (7% Mg)				
22,CC	Cement in sandstone	-2.65	+8.67	245	—	49		
38,CC*	Laminated, hard	-1.46	+9.52					
39-1, 64.5*		-0.06	+9.96					
40-3, 10*	Hard, sill contact	-8.19	-5.24	99	10	8	48	Slightly Mg-calcite
Hole 477								
15-1, 72*	Hard, sill contact	-12.16	-6.10	89	—	46	50	
Hole 475								
17-5, 121*	Dolomite cement in glauconite bed	-4.55	-11.85	34	97			

Note: * indicates duplicate stable isotope analyses. Blanks indicate no analysis, dash indicates no major peak.

as a cement within bioturbated, laminated, and transitional diatomaceous mud facies (Fig. 4). In fact, these features are best studied on the lithified samples.

Where least disturbed by drilling, the dolomitic beds commonly show a lithification gradient ranging from soft, yellowish gray, friable mudstone along outer margins to hard, impervious centers which have sonic velocities up to 5 km/s and bulk densities greater than 2.5 g/cm³ (Einsele, this volume, Pt. 2). Several other general aspects discussed in the site chapter are pertinent to dolomite formation: (1) Seismic reflectors show two possible low-angle unconformities indicating tectonic jostling of this margin during the Quaternary. (2) A zone of slightly depressed salinity from about 100 to 190 meters sub-bottom corresponds to a zone with the most abundant biogenic gas and higher rates of accumulation of terrigenous silts. This coincidence might suggest the presence of an *in situ* clathrate. (3) Heat flow is presently about 2.0 HFU; a bottom-hole temperature was measured at 49°C, and the corresponding temperature at the sediment/water interface is 9°C. Formerly higher heat flow is suggested by the state of maturation of organic matter below Core 479-39 (Deroo et al., this volume, Pt. 2). Carbon concentration increases from 360–390 meters and much of the kerogen fraction consists of pyrite. The hole was actually terminated because

of an ominous increase in thermocatagenic hydrocarbons C₁–C₈. (4) Dinoflagellates are abundant in Cores 479-27 and 479-37 and algal monocells in Cores 479-27 and 479-47. Pine pollen peaks occur in Cores 479-3, 479-17, and 479-27. These signals indicate general ranges of fluctuating climatic and oceanic conditions at the site. (5) Because of high organic (4%) and diatom frustule content, the oozes have high initial and persistent porosity (85–50%). (6) The bulk carbonate content of the hemipelagic oozes is low (0–10%), with sporadic pulselike intervals up to 25% (see LeClaire and Kelts, this volume, Pt. 2). It comprises mainly benthic foraminifer concentrations or collected laminae rich in coccoliths (Fig. 3).

Other Sites

Auxiliary carbonates recovered at other Leg 64 sites were compared with those from Site 479. At the base of Site 474, several coarse sandstone turbidites are cemented by calcite in association with a sill intrusion (Core 474A-39). At the tip of the peninsula of Baja California, a single decimeter-thick layer of yellowish gray, green-speckled mudstone was recovered at the base of the marine section in Section 475-17-5. It consists of a layer of glauconite pellet sands which are cemented by equigranular (60 μm) euhedral, limpid dolomite crys-

Table 2. Total carbon analysis by the Coulomat method.

Sample (interval in cm)	Type	Total Carbon (%)	Dolomite (%)	Calcite ^a (%)	Quartz + Feldspar ^b (%)
Hole 479					
10-6, 130	Dolomite	9.25 ^c	71 ^d	48	—
16-2, 38	Dolomite	11.57	89	66	—
16-2, 108	Dolomite	12.16	93	70	5
20-1, 100	Dolomite	11.84	91	68	—
20-3, 65	Dolomite	11.85	91	68	—
23-1, 73	Dolomite	8.37	64	45	—
29-1, 1.5-4	Dolomite	10.13	78	54	12
29-1, 4-12	Dolomite	10.99	84	64	—
29-1, 15	Dolomite	11.50	88	65	—
29,CC	Dolomite	11.47	88	65	—
32,CC	Dolomite	11.56	89	66	—
39-1, 15	Mud	2.91 (22)	None	—	58
39-1, 39	Dolomite	11.14	86	62	4
41-1, 134	Dolomite	11.63	89	66	—
42,CC	Mud	6.24	33	22	36
44-2, 45	Mud	4.10	38	8	45
44-2, 45	Mud	5.62	42	20	55
44-3, 54	Mud	5.77	39	21	19
44-3, 91	Mud	5.57	6	20	19
45,CC	Dolomite	9.13	70	47	11
45,CC	Mud	4.18	32	9	—
47-2, 116	Mud	2.19	17	None	73
47-2, 126	Dolomite	7.71	59	36	—
47-2, 134	Dolomite	11.16	85	63	—
47-2, 135	Dolomite	10.83	83	63	—
Hole 480					
19-1, 85	Mud	—	—	—	30
20-1, 10	Mud, diatom	2.10	—	—	24
31-1, 89	Mud	2.10	—	—	94
Hole 478					
1-1, 50	Mud	—	—	—	—
5-1, 139	Mg-calcite mud	—	—	50	—
22,CC	Dolomite cement ^e	45	45	—	—
38,CC	Dolomite	76	54	—	—
40-3, 10	Dolomite, contact ^e	50	50	—	—
Hole 477					
15-1, 71	Dolomite, contact ^e	40	40	—	—

^a Calcite from XRD ratio in carbonate group, calculated for %C.^b Quartz-feldspar where determined from XRD.^c Calculated on the basis of % total C and ratio of X-ray-determined dolomite/calcite/quartz.^d Calculated on the assumption of uniform 3% C_{org}.^e Samples which have no significant C_{org}.

tals, many of which have small dark centers (gas?, organic matter?, pyrite?).

Various dolomitic rocks were encountered in the Guaymas Basin. At Site 477, two samples of hard, massive, micritic dolostone were recovered from contact zones just below a dolerite sill (Section 477-15-1, and 477A-1,CC). In addition, scattered dolomite crystals and dolomite-replaced foraminifers occur in gray muds (Cores 477-15-18) as the result of high-temperature alteration of the sediment by extensive hydrothermal activity (Kelts, this volume, Pt. 2; Gieskes et al., this volume, Pt. 2). At Site 478, soft yellow clumps of magnesian calcite occur in brown oozes only 40 meters sub-bottom (Section 478-5-1). At greater depths, a coarse sandstone layer has dolomite micrite cement (Sample 478-22,CC) and a yellow gray mudstone occurs in Sample 478-39,CC. A basal contact zone with a dolerite intrusion is also marked by gray micritic dolomite (Sample 478-40,CC).

One 10-cm thick bed of light yellowish gray, massive, friable dolomitic mudstone (35% carbonate) was recovered in Section 480-20-1, 101 meters sub-bottom. Because of the proximity and the similar depth of the first occurrence of dolomite at Site 479, we at first correlated these as a contiguous bed, although this was not confirmed by the subsequent isotopic evidence.

Dredged Samples

During the course of this study, we also examined various hard, fine-grained claystones which had been dredged from various fault scarps bounding the Gulf of California Basins and interpreted as part of a Pliocene proto-Gulf sequence (Moore, 1973). Most were originally reported to be silicified diatomaceous muds because they contained identifiable foraminiferal tests. Our results show that all of the hard dredge samples from the Carmen and Guaymas sites (D-4 and D-5; Moore, 1973)

Table 3. Microprobe analyses of dolomite samples, Leg 64.

Sample Description	CaO (%)	MgO (%)	FeO (%)	SiO ₂ (%)	Al ₂ O ₃ (%)	Na ₂ O (%)	K ₂ O (%)	MnO (%)	Total (%)
479-19-1, 20 cm									
Dolomite, larger crystals	36.8	22.1	—	0.7	0.1	0.1	—	0.5	60.3
Dolomite, calcian	37.7	19.6	—	0.2	—	0.1	—	0.9	58.5
479-27,CC									
Dolomite, relict forams	36.3	21.1	—	0.4	0.1	0.3	—	—	58.2
Dolomite, foram rim	38.3	19.4	—	0.4	0.1	0.2	—	—	58.4
Dolomite, foram rim	37.2	19.3	—	0.1	—	0.1	—	—	56.8
Dolomite, foram biserial septum	36.3	20.2	—	0.2	—	0.2	—	—	57.0
Dolomite, micrite with pyrite	29.3	15.7	5.0	0.3	0.1	0.2	—	0.1	50.7
Dolomite, foram prism layer	36.3	19.4	0.1	0.7	0.1	0.1	0.1	—	56.8
479-28-1, 15 cm									
Dolomite	32.5	20.6	0.2	5.4 ^a	0.4	0.1	0.1	—	59.5
Dolomite	35.3	21.3	0.1	0.7	0.2	0.2	0.1	—	58.0
Dolomite	35.3	19.8	0.5	0.2	0.1	0.1	—	0.1	56.1
Dolomite, forams	30.2	16.7	0.4	6.5 ^a	1.2	0.2	0.3	—	55.4
479-34-5, 140 cm									
Dolomite, micrite matrix	35.3	20.6	0.1	0.8	0.2	0.2	—	—	57.2
478-22,CC									
Dolomite cement in sandstone	35.1	22.0	0.9	0.4	—	0.1	—	0.2	58.9
Stoichiometric dolomite	30.47	21.87	CO ₂ = 47.72	—	—	—	—	—	—

^a Samples possibly include relict frustules.

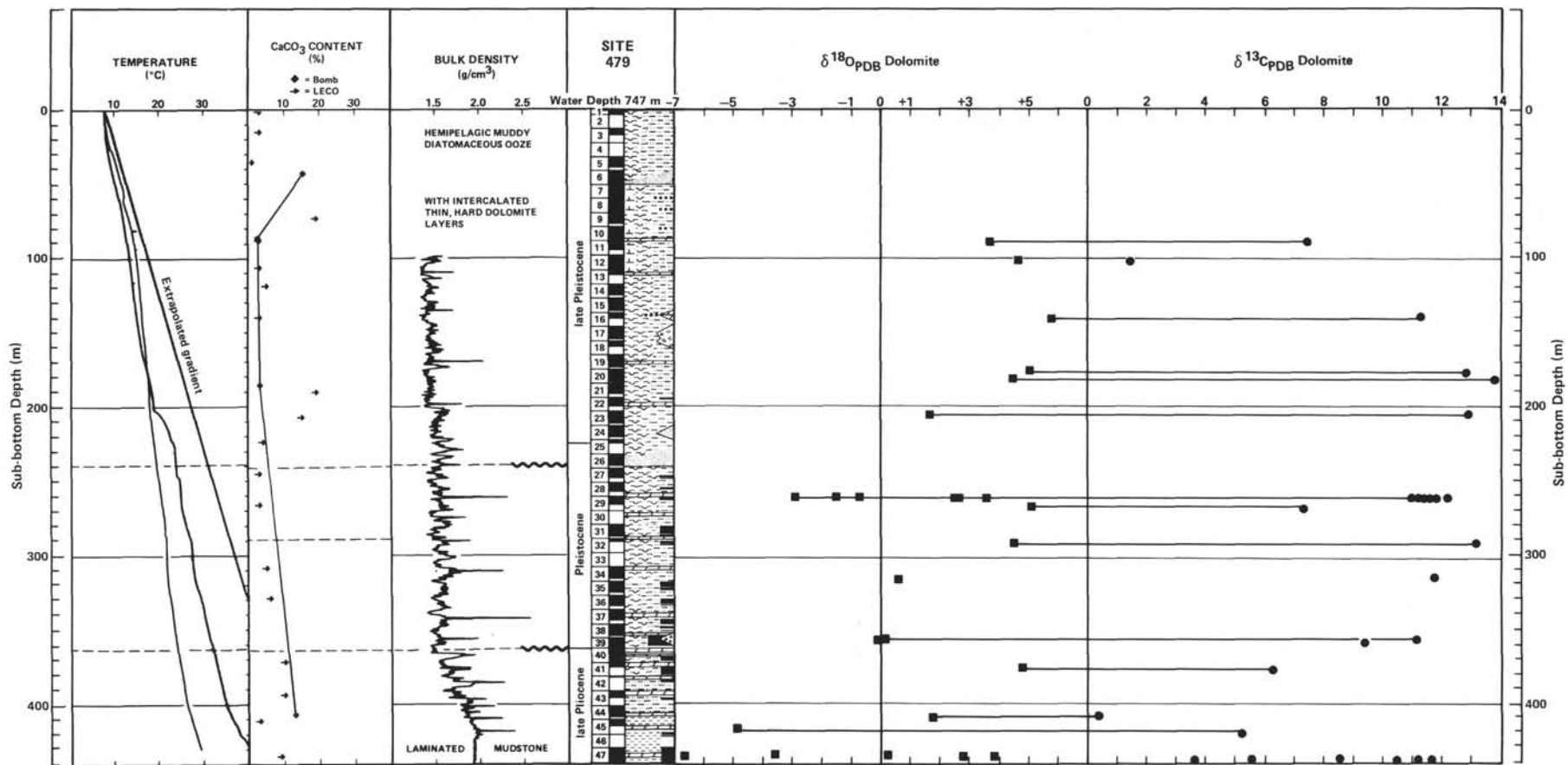


Figure 2. Hole 747 lithology, carbonate content, bulk density, and temperature logs, and the results of isotopic analysis of $\delta^{18}\text{O}$ and $\delta^{13}\text{C}$ for dolomite samples.

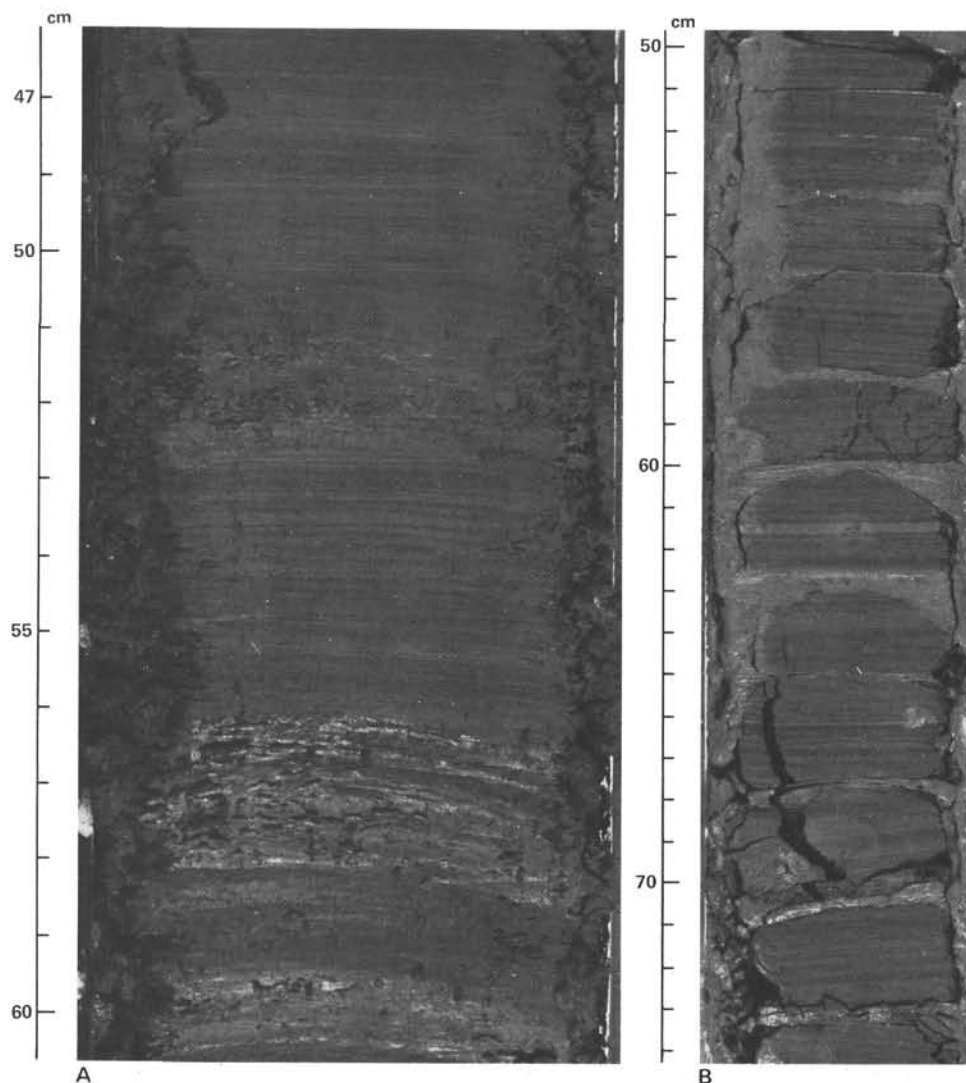


Figure 3. Examples of Hole 479 host sediments. A. Sample 479-35-5, 47–60 cm (325 m): laminated olive drab facies of muddy diatomaceous ooze (3% C_{org}) with zones of low (0–5%) and higher (10–15%) carbonate content (light laminae). B. Sample 479-47-3, 50–74 cm (437 m): hard, gray mudstone with ultrathin laminae, but without diatom frustules. Includes some rare lamellae of monospecific coccolith ooze. The biscuit texture is a drilling relict.

consist of 90–95% dolomite. Accessory minerals include quartz and, in one sample, significant clinoptilolite.

SEDIMENT PETROLOGY

The X-ray determined compositions from the (211) peak of dolomite crystals ranges from calcian-rich to stoichiometric (42–51% $MgCO_3$), and ordering peaks are weak but present (Table 1). There is a general textural trend whereby more calcian-dolomite is associated with softer samples. Most of the samples in this study fall in the range of 46–49% $MgCO_3$, and follow patterns from similar examples along the outer continental margin of Baja California (Pisciotta and Mahoney, 1981). Calcite co-existing with dolomite is a low-magnesium variety (less than 2% $MgCO_3$), as would be expected from the presence of calcareous microfossils. High-magnesian calcite (7–10% $MgCO_3$) occurs, for example, as the principal mineral in scattered, soft, yellow pellets

from the top of Hole 478 (Core 5). From the valid microprobe analyses (Table 3) none of the dolomite crystals appear to contain any significant component of iron or manganese. Pyrite, however, is an abundant accessory in both oozes and dolomite layers—an indication that dolomite formed after available iron had been locked into sulfides. Ratios of Mg/Ca from microprobe analysis are lower than those determined by XRD, because of analytical problems of inclusions, grain size, and decomposition under the electron beam, but they confirm a general excess of calcium in the crystal lattice.

Twenty-nine samples of the hemipelagic host sediment of Site 479 were also examined by routine semi-quantitative X-ray diffraction in order to determine the nature of possibly diagenetic variation of host sediment in concert with dolomitization. The relative major peak heights are used as a guide to wt.% composition for quartz, calcite, dolomite, plagioclase, K-feldspars, smec-

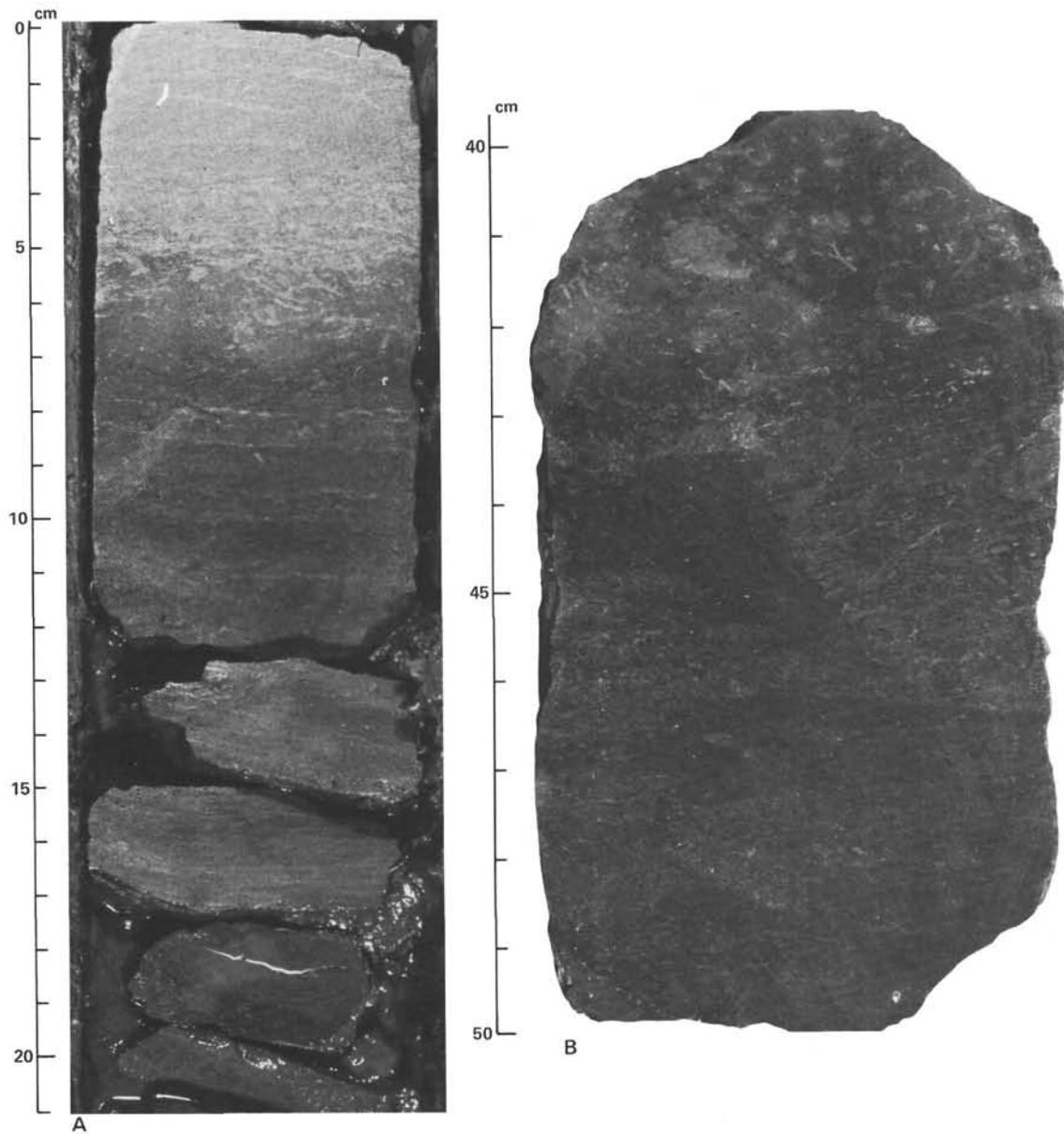


Figure 4. Core photograph examples of primary laminations and subtle textures of bioturbation which are preserved in dolomitic beds. A. Sample 479-29-1, 0-21 cm (263 m). Upper part of a bed showing a transition from laminated to burrowed facies. Brittle dolomite below 10 cm grades to firm dolomitic mudstone at the top. B. Sample 479-34-5, 40-50 cm (315 m). Moderate olive brown clayey dolomite with burrows and small pits.

tites, chlorite, micas and illite and kaolinite. In addition 7 samples were selected for a clay mineral comparison of dolomitic and nondolomitic layers. The results show that feldspars and quartz dominate (50–60%) the noncarbonate muds in approximately equal proportions. Their abundance is nearly constant throughout the holes, indicating a common, uniform, terrigenous source. Plagioclase is more common than K-feldspars. The evidence does not suggest major downhole alteration of biogenic silica to opal-CT or quartz until below 360 meters. However, clinoptilolite was detected in uniformly small quantities below 50 meters and indicates at least some active silica diagenesis. Clay minerals constitute about 15–30% of the spectrum. Illite, smectite, kaolinite, and chlorite are present, in that order of abundance. Heating indicates the presence of illite-smectite

mixed-layer varieties. Kaolinite is confirmed and a small amount of chlorite inferred from integral series of basal d-spacings. We found no obvious differences between the clay mineral spectrum of the host muds and the dolomitized beds. Carbonate minerals are minor, but include some scattered dolomite. Low-magnesian calcite persists in small amounts, sporadically, to the base of the hole, reflecting the presence of nannofossils and foraminifers. A few soft clumps of disturbed sections contain higher-magnesian calcite (2–12%). Dolomitic layers comprise up to 65% dolomite or more.

Total Carbon

In order to investigate further whether dolomite is a pore-filling cement or in addition replaces or expels components from a zone of accretion, Site 479 carbon-

ate samples were analyzed for total carbon with a Coulomat apparatus. Results are not corrected for organic carbon, which for hemipelagics in these cores is given as:

	Carbonate (%)	Organic Carbon (%)
Core 479-6	15	4
Core 479-10	3	3
Core 479-21	3	3
Core 479-44	13	3

Table 2 gives total carbon as dolomite or calcite component based on relative peak heights on XRD diagrams, again assuming a constant background organic carbon of 3%. This is too high, considering the mass differences between dolomitized and normal hemipelagic sediment, but the two figures illustrate some ranges of relative change. The results indicate that several samples exceed the amount of pore space available at shallow depths (to 80 meters) of about 60% (Einsele, this volume, Pt. 2), a fact that suggests the incorporation of precursor carbonate.

Microtextures

Both thin section (Figs. 5, 6) and SEM (Fig. 7) examination show evidence that most dolomite is present in samples as a pore-filling cement comprising individual, tiny (<10 μm) idiomorphic crystals. Diatom frustules are encased and some filled with a coarser mosaic (Fig. 5A). There is no evidence for concomitant corrosion of siliceous fossils. Dolomite micrite may, in some cases, delicately pseudomorph calcareous microfossils, as is verified by microprobe analysis of the wall of the foraminiferal test illustrated in Figure 5B. These features perhaps point to very slow, uniform processes of formation, as do the smooth, rhombohedral crystal surfaces (Fig. 7). In the siltstone sample (Fig. 6), crystals do not show evidence of successive generations of cement or even of preferred growth along prior grain boundaries.

Among different samples, we did, however, find a variety of crystal sizes and textural patterns more related to progressive degrees of induration and bed accretion than to downhole trends (Figs. 8A-F and 9A-D). Crystals range in size from 1-2 μm in softer samples containing calcian-rich, poorly crystalline (proto) dolomite. Coccoliths which coexist in these samples commonly show ragged edges, indicating some dissolution. Grain size and crystallinity increase in more indurated samples; 5 μm ranges are common. Well-formed, smooth-surfaced, sharp-edged, equigranular, interpenetrating rhombs (10-30 μm) derive from hard but punky samples which commonly have small pits that are, we believe, left from the dissolution of benthic foraminifers (Figs. 7 and 9D). Impervious hard layers then show anhedral crystal mosaics (Figs. 8F and 5C), also in the 30- μm range. None of the samples show recrystallization to a coarse sugary dolomite, common in many dolomite outcrops on land. This gradational pattern of crystal size,

abundance, stoichiometry, and habit is found on transects from edge to center on two beds (Samples 479-29-1, 0-21 cm and 479-47-3, 126-145 cm; see Figs. 4 and 9).

Stable-Isotope Results

Most of the dolomite from Sites 478 and 479 shows extreme enrichment in ^{13}C , with $\delta^{13}\text{C}$ values as great as +13.8‰ (Sample 479-20-3, 165 cm) and with an average $\delta^{13}\text{C}$ value of +9.8‰ for 30 samples. This average does not include Sample 478-40-3, 10 cm, whose negative $\delta^{13}\text{C}$ value of -5.2‰ may be related to its proximity to a sill. The general ^{13}C enrichment recorded in the dolomite is indicative of methanogenesis in the sediments at the depth of formation. The dolomite incorporates carbonate ions which are enriched in ^{13}C as a result of isotopic fractionation between carbon dioxide and methane (Bottinga, 1969). It is interesting to note that even the shallowest dolomite bed with a $\delta^{13}\text{C}$ value of +7.5‰ (Sample 479-10-6, 18 cm) demonstrates the influence of methanogenesis.

In two cases where it was possible to measure several samples across the dolomite beds, the $\delta^{13}\text{C}$ values show different patterns related to the different burial depths (Fig. 10). The 7 samples across the bed from Sample 479-29-1, 1.5 cm to Sample 479-29-1, 26.5 cm have a relatively constant $\delta^{13}\text{C}$ value with an average of +11.6‰, indicating that dolomite formation always occurred within the main zone of methanogenesis. In the case of the more deeply buried, multisampled bed (479-47-2, 126 cm to 479-47-2, 148 cm), the $\delta^{13}\text{C}$ value ranges from +11.5‰ in the center to +3.5‰ at the upper edge. We interpret this transition toward more negative values as reflecting the accretion of dolomite with increasing depth of burial. The initial dolomite with the $\delta^{13}\text{C}$ value of +11.5‰ was formed in the main zone of methanogenesis, but with time and increased burial the carbon-isotope composition of the dissolved bicarbonate became increasingly more negative. This alteration could result from the inclusion of isotopically lighter carbonate ions generated by underlying thermocatalytic decarboxylation reactions or by progressive *in situ* depletion of the heavier isotopic components in the carbonate reservoir during dolomite formation. Because the latter explanation implies a closed system that was not apparent from the constancy of the $\delta^{13}\text{C}$ values from 479-29-1, 1.5 cm to 479-2-1, 26.5 cm, the former explanation seems more plausible. It is not, however, consistent with other geochemical studies (Schoell, this volume, Pt. 2 and Galimov and Simoneit, this volume, Pt. 2), as later discussed.

The oxygen-isotope composition of the multisampled beds indicates that dolomite accretion continues with increasing depth and that the dolomite precipitates in isotopic equilibrium with the successively new burial environments. In the case of the singly sampled dolomite beds, it is difficult to interpret the significance of the oxygen-isotope ratio, because the measured value could represent any moment in the burial history of the bed. In general, the $\delta^{18}\text{O}$ value of the dolomite from Site 479 tends to include more negative values toward the lower part of the section and, overall, ranges from +5.1 to -7.4‰ (Fig. 1). A similar range was recorded in the

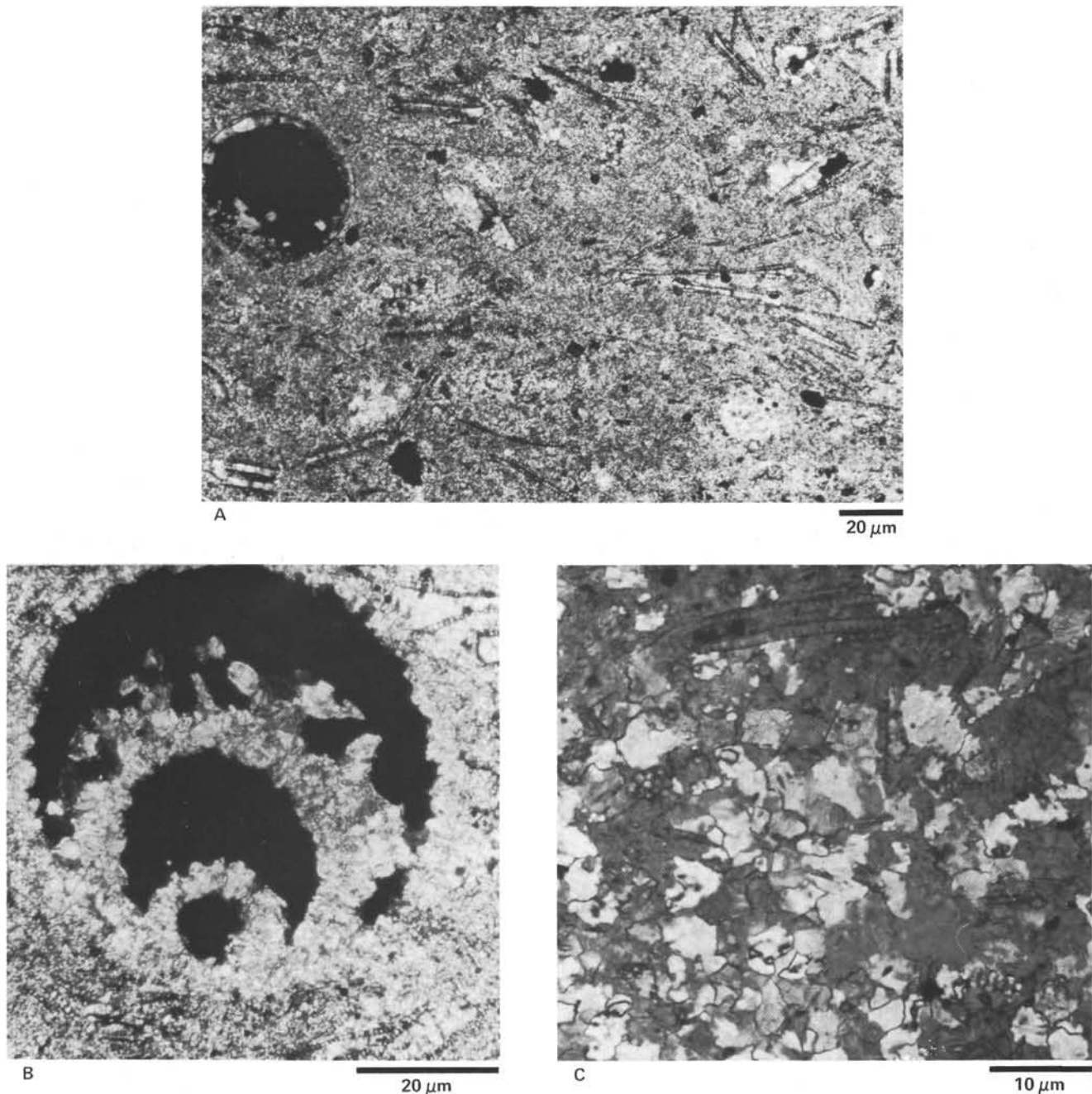


Figure 5. Thin section micrograph examples of dolomite cements, preserved diatom frustules, and relict foraminifer tests replaced by dolomite. A. Sample 479-29, CC, micrite cement. B. Sample 479-29, CC, dolomite composition of replaced foraminifers confirmed by microprobe. C. Sample 479-34-5, 50 cm, polarized crossed-nicols view of anhedral dolomite mosaic from a hard layer.

multisampled beds; it demonstrates that this isotope spread represents the possible temperature variations with depth at Site 479. In the bed from 479-29-1, 1.5 cm to 479-29-1, 26.5 cm, the more internal $\delta^{18}\text{O}$ value is +3.5‰; it progressively decreases to -2.2‰ on the external edge. A similar trend was measured for the bed from 479-47-2, 126-148 cm; the $\delta^{18}\text{O}$ value for the hard, internal sample is +3.1‰ but it progressively decreases to -7.6‰ for the friable, external sample (Fig. 10).

At Site 479, a geothermal gradient of 95.9°C/km was determined, and the ^{18}O composition of the pore waters

varied from 0‰ near the water/sediment interface to -2‰ near the base of the hole (Schoell, this volume, Pt. 2). With these two end-points, it is possible to calculate the expected ^{18}O composition of dolomite formed at any depth using the experimentally derived dolomite-water fractionation equation of Matthews and Katz (1977). The calculated $\delta^{18}\text{O}$ values can be compared with the measured values, which are believed to be representative of dolomite forming at its present location in the sediment column—that is, the dolomite nearest to the water/sediment interface (Sample 478-10-6, 18 cm)

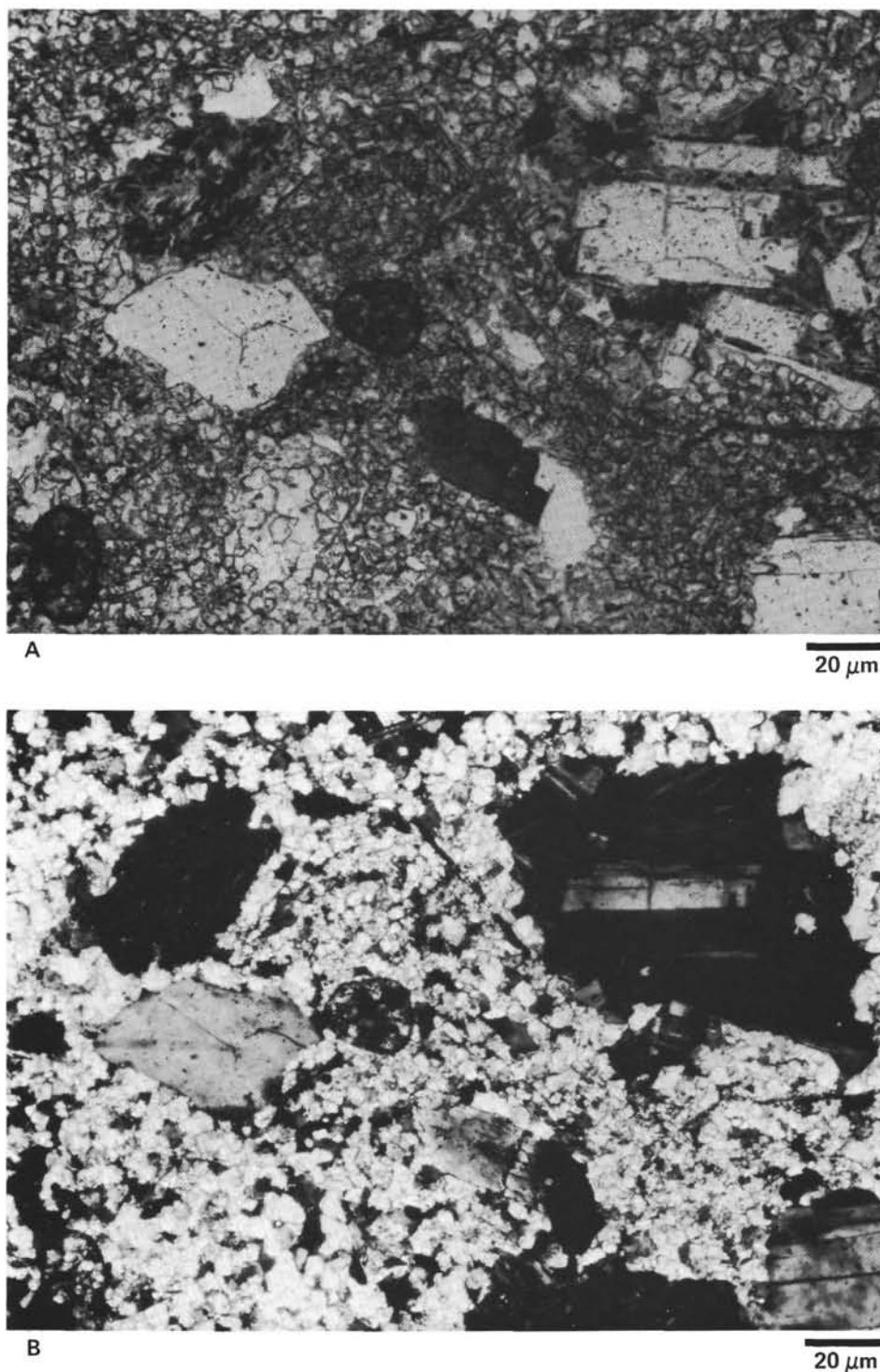


Figure 6. Thin section micrograph of dolomite micrite cementing silts from a zone which also has high concentration of biogas. Sample 479-19-1, 20 cm includes unaltered plagioclase, pieces of wood, and weathered olivine. A. Transmitted light; B. Crossed nicols.

and the outermost dolomite from the multisampled beds (479-29-1, 1.5 cm, 479-29-1, 26.5 cm, and 479-47-2, 126 cm). The calculated and measured results plus the parameters used in the calculation are compared in Table 4. The agreement between measured and calculated $\delta^{18}\text{O}$ values is reasonably good considering the many assumptions required to make the calculations. The comparison does succinctly indicate that dolomite precipitates in

isotopic equilibrium at the burial temperatures and that over time beds must continue to accrete dolomite to the individual layers.

Subsurface Nucleation

The pattern of dolomite formation in sediments from Site 479 shows petrologic, textural, and isotopic similarity with examples from Irwin et al. (1977) for the Yellow

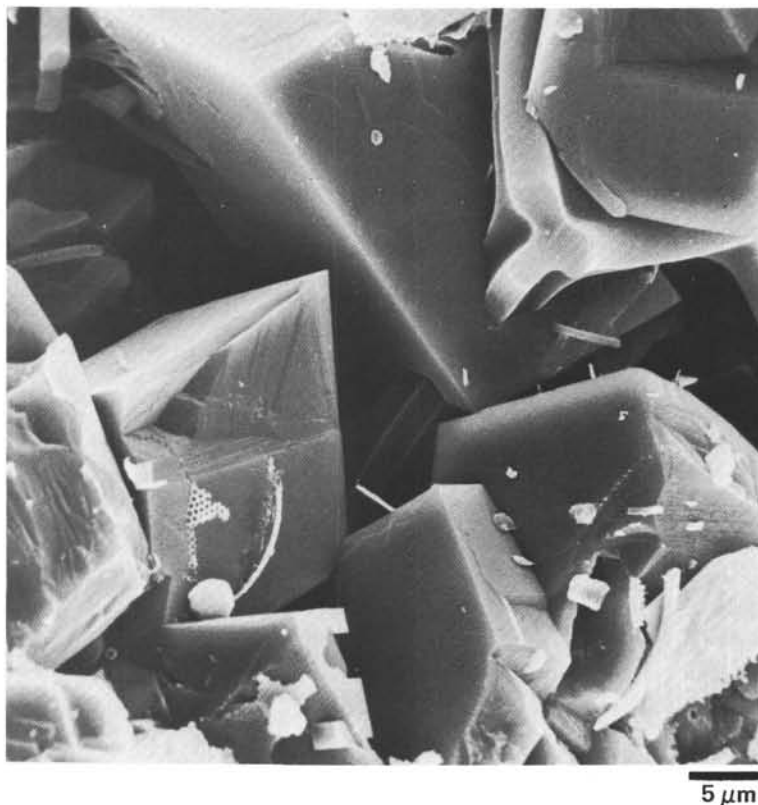


Figure 7. SEM micrograph of diagenetic interstitial dolomite crystals engulfing siliceous diatom frustules and silicoflagellate tests. Euhedral habit and smooth surfaces common to samples of firm but friable clayey dolomite (Sample 479-39-1, 37 cm; 358 m).

Ledge, Kimmeridge Clay, the Monterey Formation (Friedman and Murata, 1979), and the Leg 63 Borderland Neogene of Baja California (Pisciotta and Mahoney, 1981). These have all been interpreted in terms of depth-related diagenetic reactions in various subsurface zones of microbial metabolism. The formation of dolomite in Site 479 sediments can be considered a natural experiment in progress, and the *in situ* geochemical parameters (Fig. 11) can be related to carbonate signatures at a given depth. The rapid sedimentation rates both retain *in situ* geochemical gradients and convey a given position in the sediment column quickly, through other depth-related variables.

A comparison of the ^{13}C value of each sample with the isotopic composition of *in situ* CO_2 gas places their level of formation at depths equivalent to or shallower than their present occurrence (Fig. 11; Schoell, this volume, Pt. 2). All formed in the zone of methanogenesis, which in the Guaymas Basin and Slope begins at only a few meters sub-bottom, below the zone of sulfate reduction (see Fig. 13, later). Sulfate is quickly depleted in oozes only a few thousand years old (Goldhaber and Kaplan, 1980; and Gieskes et al., this volume, Pt. 2).

Alkalinity rises to extreme values (80 meq/l) within a few meters sub-bottom and declines uniformly down-section. This is a probable indicator of concomitant carbonate precipitation. The first dolomite identified in the oozes (60 m) and the first hard samples at 90 meters are located in zones of abrupt decrease in both calcium and

magnesium content of pore waters, suggesting that these are presently major regions of initial dolomite precipitation. Magnesium first increases slightly to 30 meters, then drops along a steep gradient from 50 to 150 meters, with an inflection around 80–100 meters (Fig. 11). Phosphate behaves in a similar manner, implying perhaps a formation of phosphates in the same zone. Gieskes et al. (this volume, Pt. 2) suggest that a rise in ammonia will add magnesium ions to pore water by exchange with smectite mixed-layer clays. In Hole 479, ammonia attains extreme values for marine sediments, and although the maximum occurs about 200 meters sub-bottom, this mechanism might provide a contributing source of magnesium for continued slow precipitation of dolomite.

Surprisingly, calcium continues to be added to pore waters with depth until a crossover point with the magnesium curve is reached at 360 meters sub-bottom. The source of this calcium is puzzling, as the high alkalinity values would indicate carbonate supersaturation in this anoxic environment. Possibly some calcium derives from the replacement of calcareous microfossils.

Accretion Rates

Evidence presented thus far strongly supports the supposition that dolomite initially precipitates in discrete zones a few tens of meters subsurface, and that during subsequent burial, centers harden while layers continue to accrete dolomite symmetrically along the margins. Isotopic evidence from the carbonates and *in*

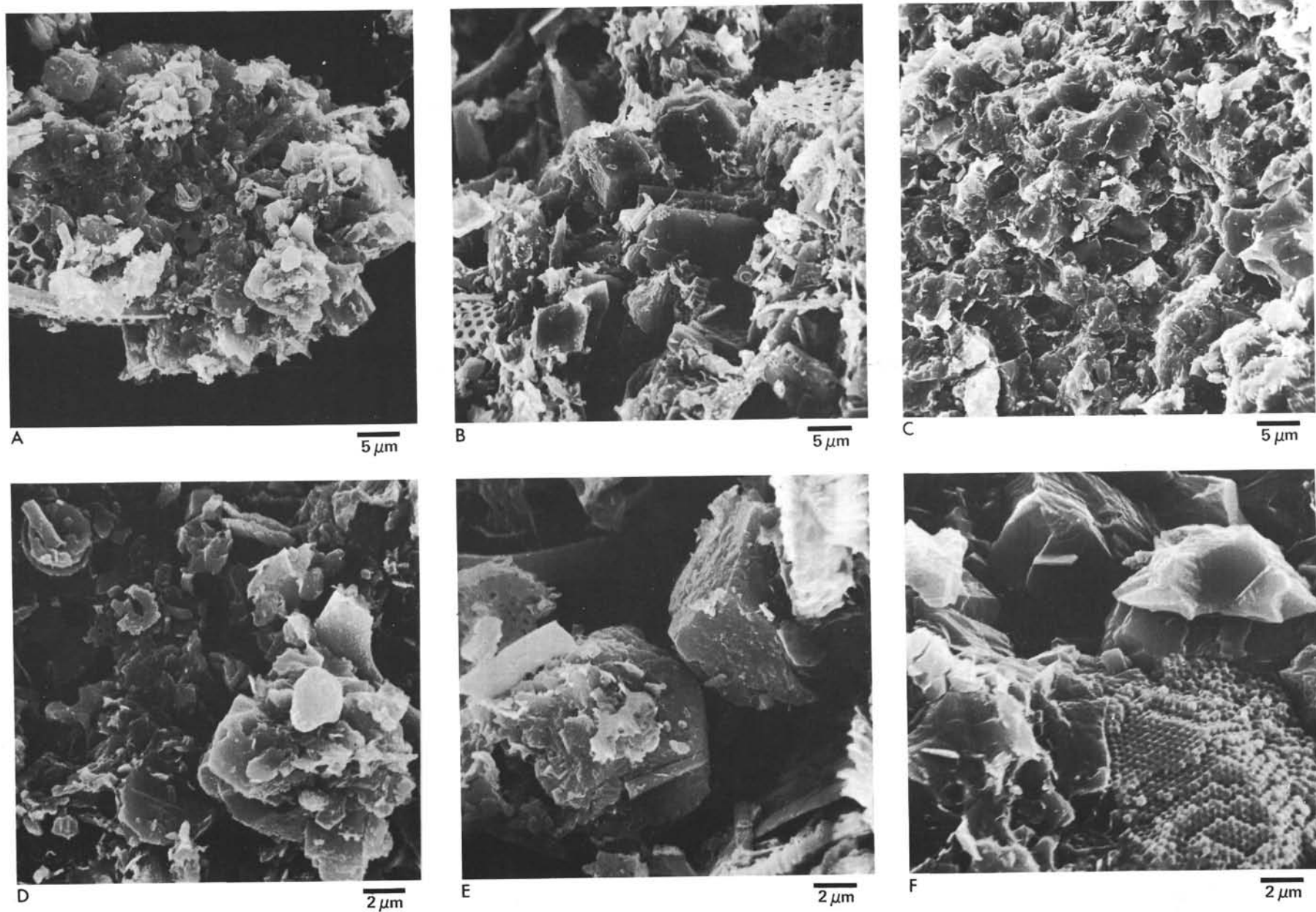


Figure 8. Examples of downhole variations of microtextures and dolomite crystal habit. A and D. Sample 479-10-6, 130 cm (88 m): soft yellow clumps with 90% calcian-dolomite and 10% calcite coccoliths in the carbonate fraction. B and E. Sample 479-23-1, 73 cm (204 m): friable sample with individual, small, poorly formed to well-formed crystals as interstitial cement; contains 8% calcite. C and F: Sample 479-47-2, 148 cm (437 m): hard compact dolomite with anastomosing, anhedral mosaic. Ordered dolomite without relict calcite or siliceous tests. Sphere aggregate is a pseudomorph of a diatom by pyrite framboids.

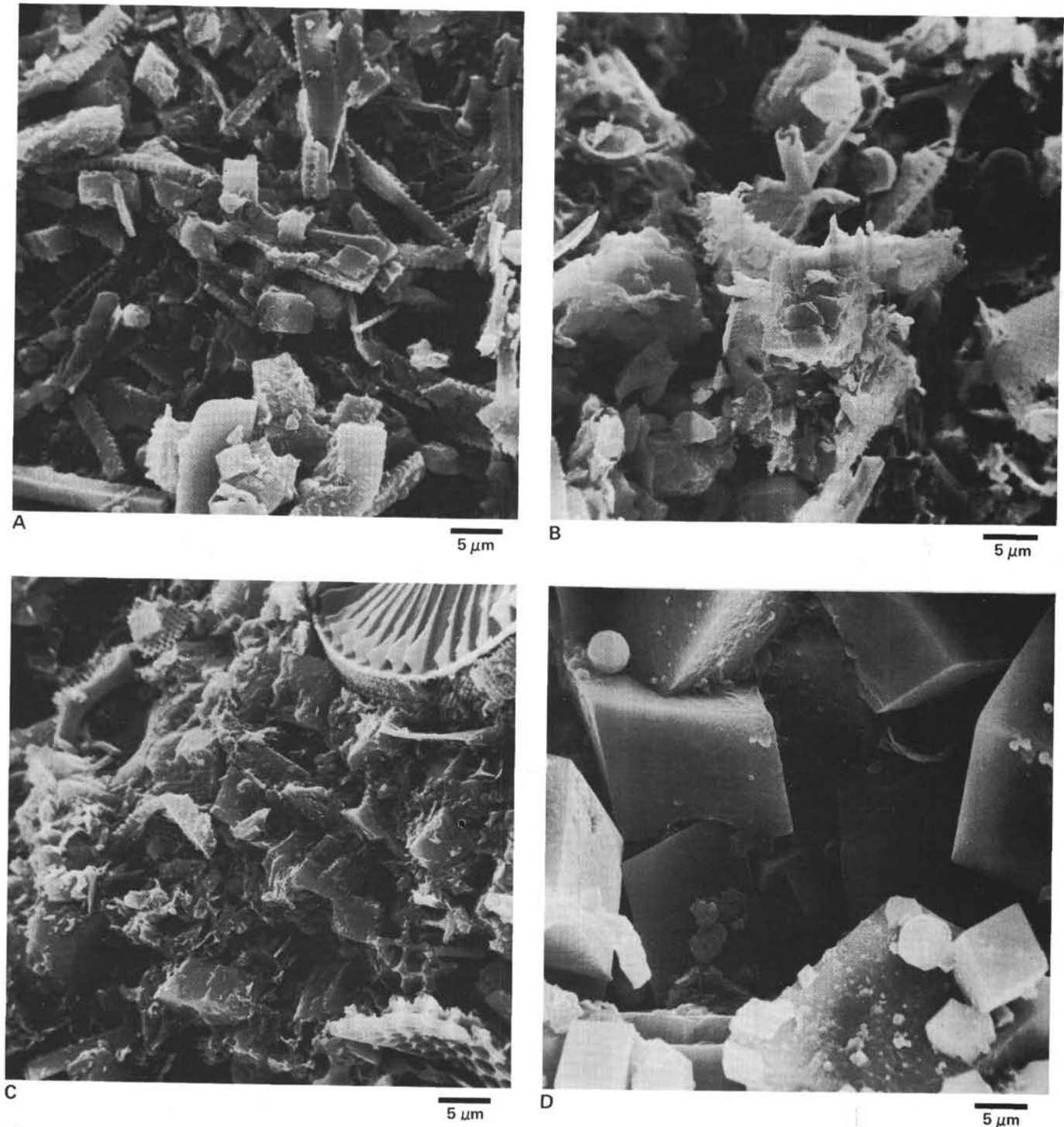


Figure 9. Same-scale comparison SEM microtextural gradations across one bed (Sample 479-29-1, 0–21 cm, 263 m; see Fig. 4). A. 1 cm: soft friable diatom mudstone with scattered 1–3- μm idiomorphic crystals. B. 4.2 cm: harder, porous dolomitic mudstone with individual poorly formed to well-formed crystals, scattered clay minerals, and organic matter. C. 24.5 cm: hard dolomitic mudstone from the lower part of the bed shows relict diatom frustules cemented by closely spaced small crystals. D. 15 cm: hard, brittle dolomite from central part of bed shows larger (10–20- μm), intergrown, euhedral rhombs.

situ gases and waters provide us with an excellent opportunity to time this process with order-of-magnitude estimates.

The lowermost bed in Section 479-47-2 (Fig. 12) is encased in hard claystone, and thus drill cores recovered at least one half of a bed relatively intact. Figure 12 shows

the upper half of this bed, which exhibits textural and mineralogical gradients from soft, laminated, calcian-dolomite mudstone at 124 cm to hard, stoichiometric dolomite with disrupted laminae at the bed center at 140 cm. The lower half was presumably crushed by drilling. We measured the isotopic composition of increment

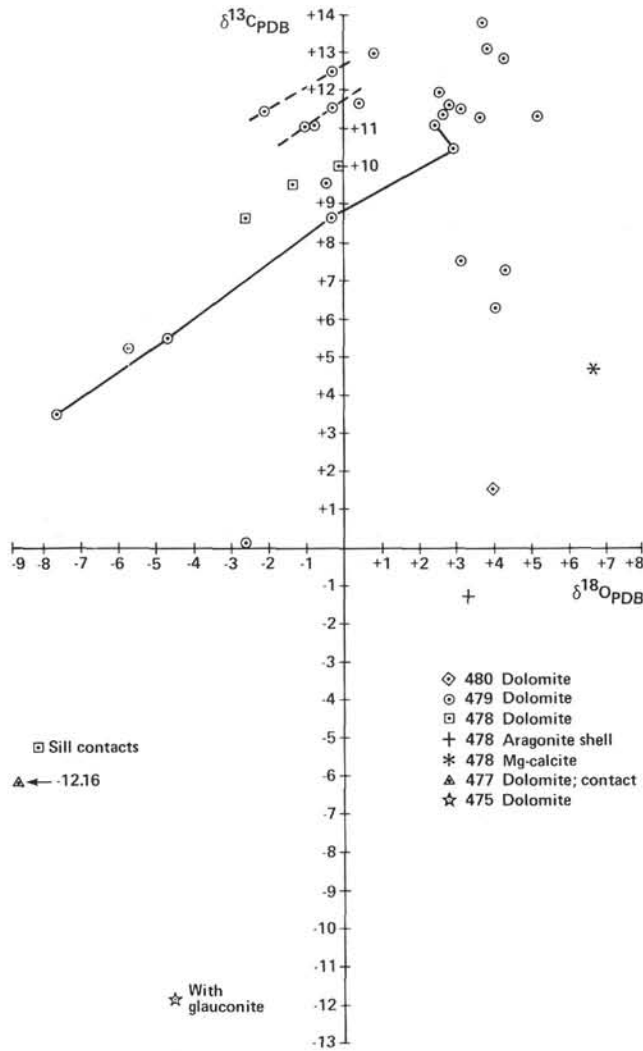


Figure 10. Plot for all isotopic measurements of $\delta^{18}\text{O}$ and $\delta^{13}\text{C}$ for dolomites of Site 479 and auxiliary samples from other sites. Lines connect trends within one bed—dashed for Core 479-29 and solid for Core 479-47.

Table 4. Calculated versus measured oxygen isotope values for diagenetic dolomite, Hole 479.

Core/Section (interval in cm)	Depth (m)	$\delta^{18}\text{O}$ SMOW (H_2O) (‰)	T (°C)	$\delta^{18}\text{O}$ PDB (Dolomite)	
				Calculated (‰)	Measured (‰)
10-6, 18	87	0	16	+3.5	+3.02
29-1, 1.5	260	-1	33	-1.5	-2.15
47-2, 126	440	-2	50	-5.8	-7.64

samples, and although both ^{18}O and ^{13}C show a wide range of values, a conspicuous linear trend in isotopic values from more positive center to more negative outer margin exists. We infer from the uniform values for 6 cm in the center that this portion formed rather quickly at approximately 80 meters sub-bottom in accordance with ^{18}O equilibria and *in situ* temperature. The linear parts of the gradients, then, represent slow, uniform accretion by diffusive processes up to 124 cm. Dolomite is probably still precipitating at the present 440 meter depth. Simple assumptions from the sedimentation rate

and ages indicate that the rate of growth is only about 0.1 to 0.6 mm/ 10^3 yr. These rates might even be high, because the calculation does not account for two minor hiatuses in the assumption of about 360 meters burial in 1–2 m.y. With such slow growth rates, diffusion of magnesium, calcium, and carbonate from over 20 meters is rapid enough to replenish the site of dolomitization. A corollary of this observation is that beds forming in areas of higher sedimentation rates will show greater ranges of values than those from slower sedimentation rate areas.

We have very little evidence to explain the episodicity of the beds, although Friedman and Murata (1979) calculated that the total available magnesium in the pore waters of such a system would support the dolomitization of only about 5% of the sedimentary section. LeClaire and Kelts (this volume, Pt. 2) have shown that there are irregular patterns of precursor carbonate present in these hemipelagic diatomaceous oozes, but some pulses up to 25% CaCO_3 occur and are indirectly linked to climate patterns in the Quaternary. Pollen evidence from the first bed of dolomite at Site 480 (Byrne, pers. comm.) suggests that it was tied to an interglacial flora. Possibly, then, such latent climate signals, in the form of slightly more than background values of precursor calcite, determine the sites in the sediment with the greatest potential for initial nucleation of dolomite.

Evidence for continued growth within the sediments at Site 479 can be used to test a hypothesis by Claypool and Kaplan (1974) which argues for reduction of CO_2 by methanogens as a prime mechanism for producing biogenic methane (Fig. 13). As methanogens reduce the CO_2 from fermentation of organic matter to CH_4 , an extreme isotopic fractionation enriches biogenic methane in ^{12}C ($\delta^{13}\text{C} = -60$ to -80‰). The remaining CO_2 reservoir becomes enriched in ^{13}C , and isotopically heavy $\delta^{13}\text{C}$ values are faithfully recorded in the diagenetic carbonate formed at that depth. A maximum should be reached; then the $\delta^{13}\text{C}$ values of both methane and total CO_2 should become lighter (see Fig. 9 in Pisciotta and Mahoney, 1981). At Site 479 we observe a transition toward lighter carbon below 100 meters for both total CO_2 and dolomite (Figs. 11 and 12). A negative shift might also be explained by the input of thermocatalytic CO_2 from below, but Schoell (this volume, Pt. 2) and Galimov and Simoneit (this volume, Pt. 2) both suggest that there is little evidence for catagenic methane. Further, the ^{13}C content of the biogenic methane remains constant below 120 meters rather than following in concert with the total CO_2 trend toward decreasing ^{13}C values. This can be simply explained as an indication that the formation of diagenetic dolomite at depth depletes a closed-system gas reservoir of ^{13}C because of isotopic fractionation between the dissolved CO_2 and the dolomite precipitate.

CONCLUSIONS

The salient features of the process model we propose (Fig. 14) interpret dolomite formation in the Gulf of California as a result of low-temperature early diagenesis, with primary precipitation of dolomite cement in interstitial spaces of anoxic, diatomaceous oozes. This

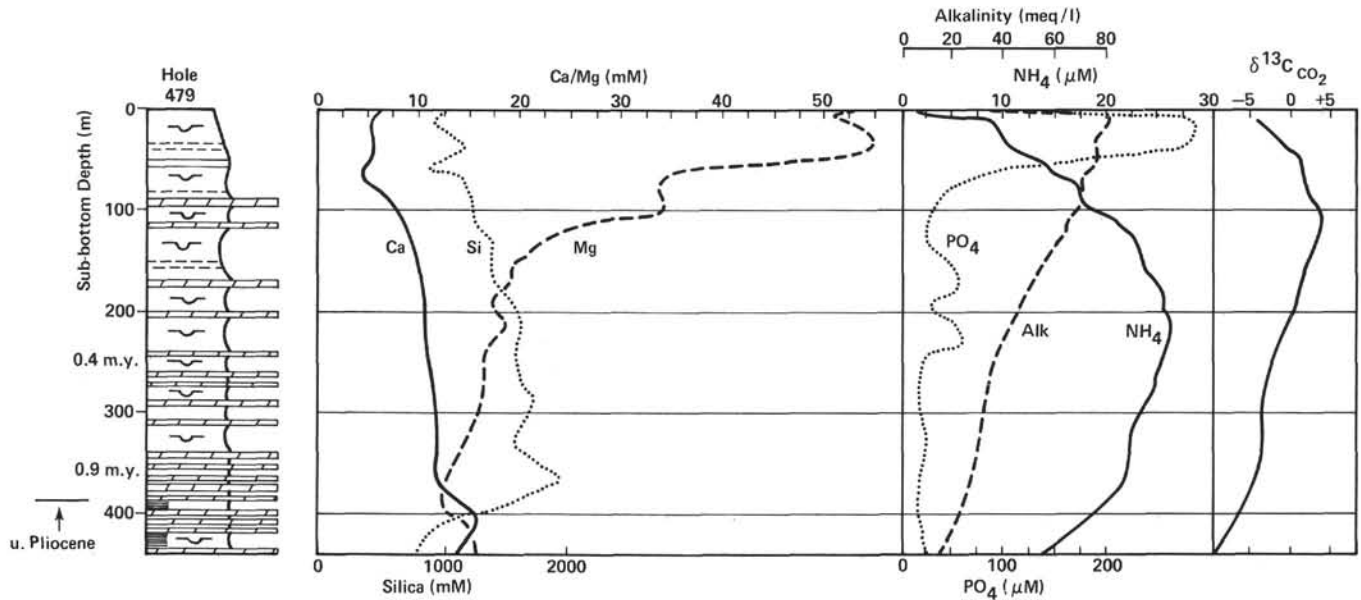


Figure 11. Summary plots of geochemical analysis from Hole 479. Ca, Si, Mg, PO₄, alkalinity, and NH₄ from shipboard determinations (site chapter, this volume, Pt. 1 and Gieskes et al., this volume, Pt. 2). Carbon-13 analysis of *in situ* dissolved CO₂ from Schoell (this volume, Pt. 2).

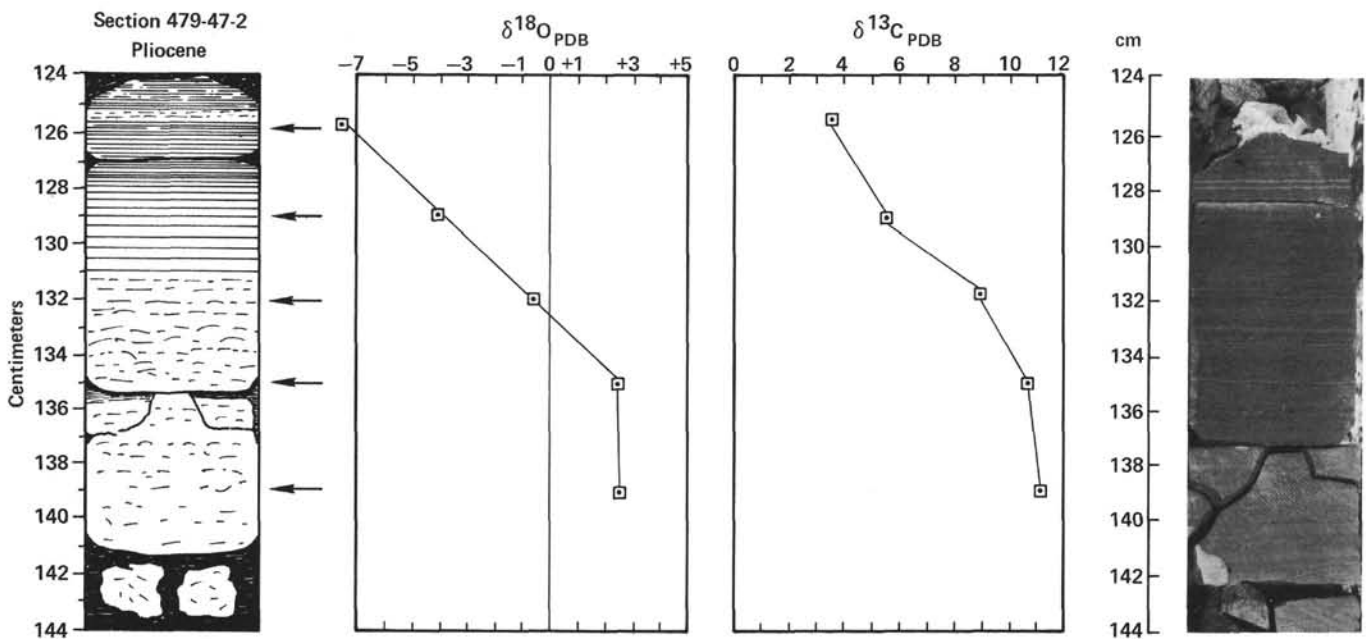


Figure 12. Linear gradients in $\delta^{18}\text{O}$ and $\delta^{13}\text{C}$ which match textural and induration trends across the upper half of the dolomite bed, Sample 479-47-2, 124-144 cm. Hard central portion at 144-134 cm and soft outer edge at the top. Note gradual inward disruption of kerogen laminae.

process takes place in a subsurface system closed to seawater exchange, characterized by low sulfate concentration, high alkalinity, and high ammonia content, commonly in conjunction with zones of methanogenesis. Elevated Mg/Ca ratios are not a limiting requirement and range from 5 to 1. The presence of a few samples with high-magnesian calcite leaves lingering doubts whether it is a necessary or coincidental precursor precipitate. We are convinced that most beds nucleate at some depth with a primary precipitate of protodolomite, and with burial continue to accrete dolomite on

both upper and lower margins in concert with slow diffusion of the necessary ions. Order-of-magnitude rates are calculated at 0.6 mm/10³ yr. Dolomite crystals at the bed centers grow, coalesce, and mature, but their retention of isotope signals from shallow depths suggests that this occurs quickly or without further isotopic exchange. We do not see evidence for relict centers of calcian-dolomite; this is puzzling, but perhaps suggests uniform, linear, growth patterns.

Although this type of dolomite formation is not volumetrically important, it has significant environmental

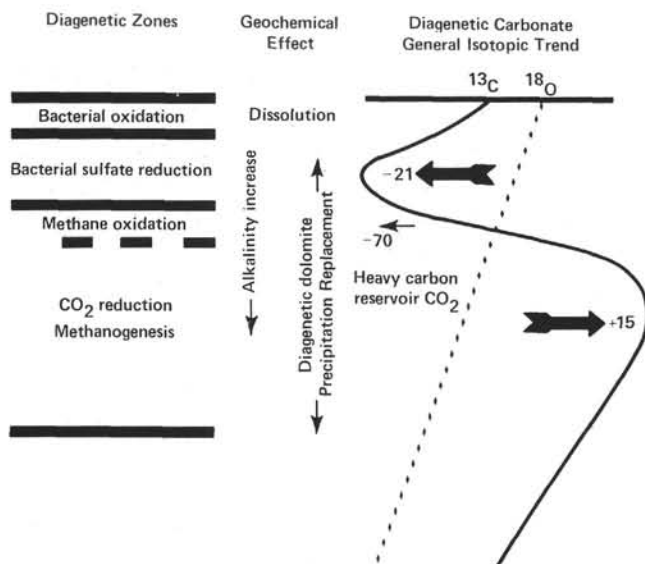


Figure 13. Schematic model of diagenetic zones in anoxic sediments and hypothetical trends in isotopic composition of diagenetic carbonates formed at various sub-bottom depths (after Claypool and Kaplan, 1974; Irwin et al., 1977; Irwin, 1980; and Pisciotta and Mahoney, 1981). Carbon released by oxidation of methane could lead to very negative signatures in carbonates formed in this zone, but none were encountered in Leg 64.

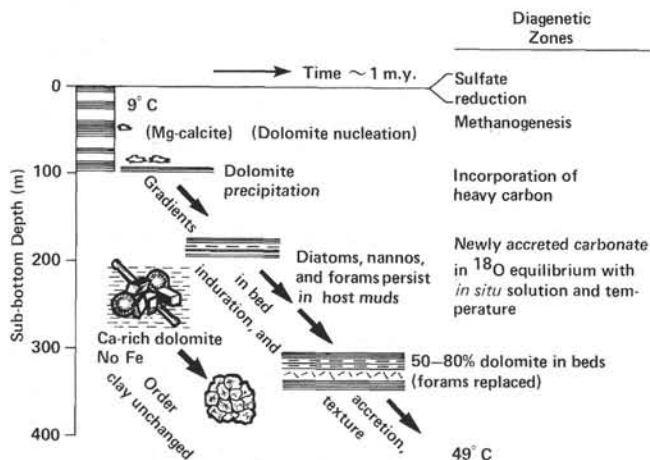


Figure 14. Summary model from Site 479 for nucleation and slow accretion of dolomite layers with subsequent burial. Concomitant gradients occur in texture, mineralogy, and isotopic composition.

implications for the geologic record. Because it is an early diagenetic feature in soft sediments, primary sedimentary structures and even microfossils are more likely to survive compaction and later diagenesis. Paleomagnetic directions, for example, should show less inclination error. We note that although heavy carbon is one of the clearest evidences for this mechanism, paleoenvironmental or paleotemperature interpretations from isotopic signals are suspect if based only on a single sample from such beds.

In terms of hydrocarbon potential, dolomite beds may hinder or guide the migration of biogenic gases in particular, as mentioned by Pisciotta and Mahoney

(1981), Irwin (1980), and Kelts and McKenzie (1980). With increasing compaction, such beds are brittle and may brecciate to form reservoir rocks within a sequence of ideal source beds.

Diagenetic carbonates are now known to be widespread in modern hemipelagic, argillaceous, anoxic sediments of continental margin settings (Pisciotta and Mahoney, 1981; Wada, et al., 1982; Matsumoto and Iijima, 1980), and are thus likely to be part of the geologic record where such settings are now part of orogenic belts. Puzzling dolomite beds, probably of similar origin, do occur, for example in the Mesozoic Schiste Lustré of the Swiss Alps (e.g., Frisch, 1980; Kelts, 1981). These in the past required complex tectonic interpretations to be consistent with the reigning theories of dolomite formation in evaporite or meteoric environments. Perhaps these and other occurrences should be reevaluated in light of the environments of formation for deep sea dolomite.

ACKNOWLEDGMENTS

Our interest in anoxic carbonates was greatly stimulated by discussions with K. Pisciotta, J. Gieskes, M. Schoell and M. A. Arthur. For technical assistance, we thank U. Gerber for photographs, H. U. Franz for SEM, G. Eberli for Coulomat analysis, and Kathy Sanderson for illustrations. K. K. is particularly grateful to DSDP for the opportunity to have participated in DSDP cruise Leg 64. We appreciate support from the Swiss National Science Foundation and from JOIDES for travel. Our special thanks to F. Mélières, R. Létolle, and H. Weissert for their reviews and criticisms.

REFERENCES

- Baker, P., and Kastner, M., 1981. Constraints on the formation of sedimentary dolomite. *Science*, 213:214-216.
- Berger, W. H., and von Rad, U., 1972. Cretaceous and Cenozoic sediments from the Atlantic Ocean. In Hayes, D. E., Pimm, A. C., et al., *Init. Repts. DSDP*, 14: Washington (U.S. Govt. Printing Office), 787-954.
- Bottinga, Y., 1969. Calculated fractionation factors for carbon and hydrogen isotope exchange in the system calcite-carbon dioxide-graphite-methane-hydrogen-water vapor. *Geochim. Cosmochim. Acta*, 33:49-64.
- Bramlette, M. N., 1946. *The Monterey Formation of California and the Origin of Its Siliceous Rocks*. U.S. Geol. Surv. Prof. Paper 212.
- Calvert, S., 1966. Origin of diatom-rich varved sediments from the Gulf of California. *J. Geol.*, 76:546-565.
- Claypool, G. E., and Kaplan, I. R., 1974. The origin and distribution of methane in marine sediments. In Kaplan, I. R. (Ed.), *Natural Gases in Marine Sediments*: New York (Plenum), pp. 99-139.
- Craig, H., 1957. Isotopic standards for carbon and oxygen and correction factors for mass spectrometric analysis of carbon dioxide. *Geochim. Cosmochim. Acta*, 12:133-149.
- Deuser, W. G., 1970. Extreme $^{13}\text{C}/^{12}\text{C}$ variations in Quaternary dolomites from the continental shelf. *Earth Planet. Sci. Lett.*, 8: 118-124.
- Friedman, I., and Murata, K. J., 1979. Origin of dolomite in Miocene Monterey Shale and related formations of the Tremblor Range, California. *Geochim. Cosmochim. Acta*, 43:1357-1365.
- Frisch, W., 1980. Post-Hercynian formations of the western Tauern window: Sedimentological features, depositional environment, and age. *Mitt. Oestrr. Geol. Ges.*, 71/72:49-63.
- Garrison, R. E., 1981. Pelagic and hemipelagic sedimentation in active margin basins. *Depositional Systems of Active Continental Margin Basins: Short Course Notes*. Soc. Econ. Paleontol. Mineral. Pacific Sect., pp. 15-38.
- Goldhaber, M., and Kaplan, I. R., 1980. Mechanisms of sulfur incorporation and isotope fractionation during early diagenesis in sediments of the Gulf of California. *Marine Chemistry*, 9:95-144.

- Hathaway, J. C., and Degens, E. T., 1969. Methane-derived marine carbonates of Pleistocene age. *Science*, 165:690-692.
- Hein, J. R., O'Neil, J. R., and Jones, M. G., 1979. Origin of authigenic carbonates in sediment from the deep Bering Sea. *Sedimentology*, 26:681-705.
- Irwin, H., 1980. Early diagenetic carbonate precipitation and pore fluid migration in the Kimmeridge Clay of Dorset, England. *Sedimentology*, 27:577-591.
- Irwin, H., Curtis, C., and Coleman, M., 1977. Isotopic evidence for source of diagenetic carbonates formed during burial of organic-rich sediments. *Nature*, 269:209-213.
- Kelts, K. R., 1981. A comparison of some aspects of sedimentation and translational tectonics from the Gulf of California and the Mesozoic Tethys, Northern Peninic Margin. *Eclog. Geol. Helv.*, 74:317-338.
- Kelts, K. R., and McKenzie, J. A., 1980. Formation of deep-sea dolomite in anoxic diatomaceous oozes. *26 Int. Geol. Congr. Paris, Fr.*, 1:244. (Abstract)
- Land, L. S. 1980. The isotopic and trace element geochemistry of dolomite: The state of the art. In Zenger, D. H., Dunham, J. B., Ethington, R. L., *Concepts and Models of Dolomitization*: Soc. Econ. Paleontol. Mineral. Spec. Pub. 28:87-110.
- McKenzie, J. A., Jenkyns, H. C., and Bennet, G. G., 1980. Stable isotope study of the cyclic diatomite-claystones from the Tripoli Formation, Sicily: A prelude to the Messinian salinity crisis. *Paleogeogr. Paleoclimatol. Paleocol.*, 29:125-141.
- McCrea, J. M., 1950. On the isotopic chemistry of carbonates and a paleotemperature scale. *J. Chem. Phys.*, 18:849-857.
- Matthews, A., and Katz, A., 1977. Oxygen isotope fractionation during the dolomitization of calcium carbonate. *Geochim. Cosmochim. Acta*, 41:1431-1438.
- Matsumoto, R., and Iijima, A., 1980. Carbonate diagenesis in Cores from Sites 438 and 439 off Northeast Honshu, Northwest Pacific, Leg 57, Deep Sea Drilling Project. In Scientific Party, *Init. Repts. DSDP*, 56, 57, Pt. 2: Washington (U.S. Govt. Printing Office), 1117-1131.
- Moore, D. G., 1973. Plate-edge deformation and crustal growth, Gulf of California structural province. *Geol. Soc. Am. Bull.*, 84: 1883-1906.
- Murata, K. J., Friedman, I., and Madsen, B. M., 1969. *Isotopic Composition of Diagenetic Carbonates in Marine Miocene Formations of California and Oregon*. U.S. Geol. Surv. Prof. Paper 614-B.
- Pisciotta, K. A., 1981. Review of secondary carbonates in the Monterey Formation, California. *The Monterey Formation and Related Siliceous Rocks of California*. Soc. Econ. Paleontol. Mineral. Spec. Publ., pp. 273-283.
- Pisciotta, K. A., and Mahoney, J. J., 1981. Isotopic survey of diagenetic carbonates, Deep Sea Drilling Project Leg 63. In Yeats, R. S., Haq, B. U., et al., *Init. Repts. DSDP*, 63: Washington (U.S. Govt. Printing Office), 595-609.
- Russell, K. L., Deffeyes, K. S., Fowler, G. A., et al., 1967. Marine dolomite of unusual isotopic composition. *Science*, 130:1658-1659.
- Sharma, T., and Clayton, R. N., 1965. Measurement of $^{18}\text{O}/^{16}\text{O}$ ratios of total oxygen of carbonates. *Geochim. Cosmochim. Acta*, 29:1347-1353.
- Spotts, J. H., and Silverman, S. R., 1966. Organic dolomite from Point Fermin, California. *Am. Mineral.*, 51:1144-1155.
- Supko, P. R., Stoffers, P., and Coplen, T. B., 1974. Petrography and geochemistry of Red Sea dolomite. In Whitmarsh, R. B., Weser, O. E., Ross, D. A., et al., *Init. Repts. DSDP*, 23: Washington (U.S. Govt. Printing Office), 867-878.
- Wada, H., Niitsuma, N., Nagasawa, K., and Okada, H., 1982. Deep sea carbonate nodules from the Middle America Trench area off Mexico, Deep Sea Drilling Project Leg 66. In Watkins, J. S., Moore, J. C., et al., *Init. Repts. DSDP*, 66: Washington (U.S. Govt. Printing Office), 453-474.